of a predoctoral fellowship for T.R.C.

Appendix A

$Ru(NH{=}CH{-}CH{=}NH)_2(O)_2^{2+}$ Geometry. A. Glyoxal Diimine.[14] The bond lengths and bond angles for the glyoxal diimine ligands were taken from those of bipyridine. R(N—H) = 1.0 Å; R(C—H) = 1.09 Å; R(N=C) = 1.35 Å; R(C—C) = 1.50 Å; θ(N—C—C) = 116.1°.

B. Other. The Ru-N bond lengths were chosen to be the same as those found to be the equilibrium value in the INDO/1 geometry optimization of $[Ru(NH{=}CH{-}CH{=}NH)_2(NH_3)(O)]^{2+}$, i.e. ≈2.1 Å. This gives good agreement with the experimental values of 2.17-2.24 Å for Ru(VI)-dioxo complexes with nitrogen ligands reported by Che et al.[5e] The equilibrium Ru-O bond lengths were determined by varying both Ru-O bonds simultaneously (by the same amount) while the geometry of the rest of the complex was kept fixed. The equilibrium value of 1.71 Å obtained is in excellent agreement with the values of 1.71-1.72 Å obtained by Che and co-workers for Ru(VI)-dioxo complexes.[5e] R(Ru—N) = 2.06 Å; R(Ru=O) = 1.71 Å.

Contribution from the Department of Chemistry, Michigan State University, East Lansing, Michigan 48824, and the Arthur Amos Noyes Laboratory,† California Institute of Technology, Pasadena, California 91125

Luminescence from Diplatinum(III) Tetraphosphate Complexes: Dynamics of Emissive $d\sigma^*$ Excited States

Yeung-gyo K. Shin,‡ Vincent M. Miskowski,*,§ and Daniel G. Nocera*,‡,∥

Received December 27, 1989

Solids and low-temperature solution glasses of the diplatinum(III) tetraphosphates $Pt_2(HPO_4)_4L_2^{n-}$ (L = H_2O, n = 2; L = Cl or Br, n = 4) exhibit red luminescence upon irradiation with near-ultraviolet light. Emission lifetimes and quantum yields of crystalline potassium salts were measured over a wide temperature range (10-300 K). Room-temperature lifetimes of 0.33, 0.71, and 0.39 μs for the axially substituted aquo, chloro, and bromo $Pt^{III}_2L_2$ tetraphosphates, respectively, increase dramatically with decreasing temperature. The temperature dependence of the lifetime is derived from the thermal population of a nonemissive state energetically proximate to a lowest energy emissive excited state of $d\sigma^*$ character (ΔE = 1126, 2256, and 2117 cm^{-1} for the $Pt^{III}_2(H_2O)_2$, $Pt^{III}_2Cl_2$, and $Pt^{III}_2Br_2$ tetraphosphate complexes, respectively). Temperature-dependent quantum yield measurements in conjunction with lifetime data reveal that the nonradiative decay rate constant of the upper excited state is 10^2-10^4 greater than that of the emissive excited state. Spectroscopic analysis of electronic absorption, excitation, and emission spectra is consistent with an excited-state model in which the emissive state is assigned to the ($B_{1u}(^3E_u)$, $B_{2u}(^3E_u)$) spin-orbit component of the $^3(d\pi^*d\sigma^*)$ configuration, and the higher energy deactivating excited state is the $E_u(^3E_u)$ spin-orbit component.

Introduction

The lowest energy electronic transitions of many singly bonded metal-metal (M-M) complexes involve the population of the $d\sigma^*$ metal-metal level.[1-4] Typically, significant weakening of the metal-metal interaction results upon promotion of an electron to the $d\sigma^*$ orbital, and not surprisingly, photoinduced cleavage of the metal-metal bond has emerged as the dominant excited-state decay pathway of M-M species.[5-16] The d^7-d^7 dimer $Mn_2(CO)_{10}$ is the cornerstone example of such a photochemical process. Excitation into the dimer's absorption manifold, which is dominated by the intense $d\sigma$-$d\sigma^*$ absorption band and weaker $d\pi$-$d\sigma^*$ band to lower energy,[17] leads to cleavage of the Mn-Mn bond to yield neutral $\cdot Mn(CO)_5$ radical fragments.[18-24] Because $d\sigma^*$ deactivation pathways are extremely efficient, the lifetimes of electronically excited M-M complexes are short,[25] and luminescence from M-M complexes is rare. To this end, coordination of M-M cores by bridging ligands will prevent metal-metal dissociation and the expectation of luminescence from M-M complexes is a reasonable one. Indeed recent observations of luminescence from diplatinum(III) pyrophosphite complexes, $Pt_2(pop)_4X_2^{4-}$ (pop = $(HO_2P)_2O$, X = halide),[26] a binuclear dirhodium(II,0) fluorophosphine complex, $Rh_2[(F_2P)_2N(CH_3)]_3(PF_3)Cl_2$,[27] and bidentate phosphine derivatives of $Re_2(CO)_{10}$[28] represent the first examples of $d\sigma^*$ luminescence. These complexes contain bridging ligands with only one bridgehead atom, and thus, deactivation by metal-metal bond cleavage in the excited state is circumvented. However, although retention of the M-M core in the excited state is a necessary condition of $d\sigma^*$ luminescence, it is not sufficient. The paucity of emissive M-M complexes despite the synthesis of several bridged complexes during the past years suggests that subtler, less well understood perturbations play an important role in the deactivation of $d\sigma^*$ excited states.

† Contribution No. 7927.
‡ Michigan State University.
§ California Institute of Technology.
∥ Alfred P. Sloan Fellow and Presidential Young Investigator.

(1) (a) Miskowski, V. M.; Schaefer, W. P.; Sadeghi, B.; Santarsiero, B. D.; Gray, H. B. *Inorg. Chem.* **1984**, *23*, 1154. (b) Miskowski, V. M.; Smith, T. P.; Loehr, T. M.; Gray, H. B. *J. Am. Chem. Soc.* **1985**, *107*, 7925.
(2) Albright, T. A.; Burdett, J. K.; Whangbo, M.-H. *Orbital Interactions in Chemistry*; Wiley-Interscience: New York, 1985; Chapter 17.
(3) Levenson, R. A.; Gray, H. B. *J. Am. Chem. Soc.* **1975**, *97*, 6042.
(4) Harvey, P. D.; Butler, I. S.; Barreto, M. C.; Coville, N. J.; Harris, G. W. *Inorg. Chem.* **1988**, *27*, 639.
(5) Meyer, T. J.; Casper, J. V. *Chem. Rev.* **1985**, *85*, 187.
(6) Geoffroy, G. L.; Wrighton, M. S. *Organometallic Photochemistry*; Academic Press: New York, 1979.
(7) Wrighton, M. S.; Graff, J. L.; Luong, J. C.; Reichel, C. L.; Robbins, J. L. In *Reactivity of Metal-Metal Bonds*; Chisholm, M. H., Ed.; ACS Symposium Series 155; American Chemical Society: Washington, DC, 1981; p 85.
(8) (a) Rushman, P.; Brown, T. L. *J. Am. Chem. Soc.* **1987**, *109*, 3632. (b) Lee, K.-W.; Brown, T. L. *J. Am. Chem. Soc.* **1987**, *109*, 3269. (c) Lee, K.-W.; Brown, T. L. *Inorg. Chem.* **1987**, *26*, 1852.
(9) (a) Vaida, V. In *High-Energy Processes in Organometallic Chemistry*; Suslick, K. S., Ed.; ACS Symposium Series 333; American Chemical Society: Washington, DC, 1987; p 70. (b) Hollingsworth, W. E.; Vaida, V. *J. Phys. Chem.* **1986**, *90*, 1235.
(10) Wuu, Y.-M.; Zou, C.; Wrighton, M. S. *J. Am. Chem. Soc.* **1987**, *109*, 5861.
(11) (a) Metcalf, P. A.; Kubiak, C. P. *J. Am. Chem. Soc.* **1986**, *108*, 4682. (b) Reinking, M. K.; Kullberg, M. L.; Cutler, A. R.; Kubiak, C. P. *J. Am. Chem. Soc.* **1985**, *107*, 3517.
(12) Isobe, K.; Kimura, S.; Nakamura, Y. *J. Organomet. Chem.* **1987**, *331*, 221.
(13) Yasufuku, K.; Hiraga, N.; Ichimura, K.; Kobayashi, T. In *Photochemistry and Photophysics of Coordination Compounds*; Yersin, H., Vogler, A. Eds.; Springer-Verlag: New York, 1987; p 271.
(14) Veillard, A.; Dedieu, A. *Nouv. J. Chim.* **1983**, *7*, 683.
(15) (a) Herrick, R. S.; Brown, T. L. *Inorg. Chem.* **1984**, *23*, 4550. (b) Walker, H. W.; Herrick, R. S.; Olsen, R. J.; Brown, T. L. *Inorg. Chem.* **1984**, *23*, 3748. (c) Wegman, R. W.; Brown, T. L. *Inorg. Chem.* **1983**, *22*, 183.
(16) Bohling, D. A.; Gill, T. P.; Mann, K. R. *Inorg. Chem.* **1981**, *20*, 194.
(17) Levenson, R. A.; Gray, H. B.; Ceasar, G. P. *J. Am. Chem. Soc.* **1970**, *92*, 3653.
(18) (a) Prinslow, D. A.; Vaida, V. *J. Am. Chem. Soc.* **1987**, *109*, 5097. (b) Leopold, D. G.; Vaida, V. *J. Am. Chem. Soc.* **1984**, *106*, 3720.

0020-1669/90/1329-2308$02.50/0

Owing to our interest in the properties of $d\sigma^*$ excited states[26-28] and in excited-state chemistry of binuclear metal phosphate complexes,[29] we have undertaken photophysical investigations of the metal–metal single-bonded $Pt_2(HPO_4)_4L_2^{n-}$ (L = H_2O, n = 2; L = Cl or Br, n = 4) complexes whose structure consists of the symmetrical disposition of phosphate ligands about the Pt^{III}_2 core with donor ligands L occupying axial coordination sites.[30] Typical of most d^7–d^7 complexes, an intense band attributable to the population of the $d\sigma^*$ level dominates the electronic absorption spectrum of $Pt^{III}_2(HPO_4)_4L_2^{n-}$ complexes. We now report that solids and low-temperature glasses of $Pt^{III}_2(HPO_4)_4L_2^{n-}$ complexes exhibit intense red luminescence upon irradiation into the ultraviolet and visible absorption manifolds and that luminescence persists even at higher temperature. A striking observation is the marked temperature dependence of the luminescence intensity and emission lifetime. In an effort to identify the factors important in mediating this temperature dependence, the photophysical properties of the $Pt^{III}_2(HPO_4)_4L_2^{n-}$ complexes have been studied over a wide temperature range. Interpretation of this temperature dependence in the context of d^7–d^7 electronic structural considerations has provided us with the first insight into the deactivating pathways of *emissive* $d\sigma^*$ excited states.

Experimental Section

Synthesis of Compounds. The $Pt^{III}_2(HPO_4)_4L_2^{n-}$ complexes were prepared with a slight modification of literature methods.[31,32] A suspension of $Pt(NH_3)_2(NO_2)_2$ (0.5 g, 1.6 mmol) in 85% H_3PO_4 (15 mL) was heated to 100.0 ± 1.0 °C. The progress of the reaction was followed by visually monitoring the brown fumes of NO_2 released from solution. Upon the cessation of NO_2 liberation, K_2HPO_4 (0.7 g, 4.0 mmol in 5 mL of H_2O) was added with stirring to the cooled solution. The yellow precipitate that formed after 1 h was collected, washed with ethanol and ether, and air-dried. Crystalline $K_2Pt_2(HPO_4)_4(H_2O)_2$ was obtained from an aqueous solution of the complex by slow evaporation of the solvent. The halide derivatives were prepared by the addition of aqueous solution saturated with potassium halide to a solution of $K_2Pt_2(HPO_4)_4(H_2O)_2$ in water. Slow evaporation of water from solutions containing the aquo complex and a 100 molar excess of the appropriate potassium halide yielded pure crystalline samples. The $Pt^{III}_2(HPO_4)_4L_2^{n-}$ products were characterized by UV–vis absorption and ^{31}P NMR spectroscopy. It is noteworthy, in the context of this study, that luminescent impurity ions coprecipitated with $K_nPt_2(HPO_4)_4L_2$ (L = H_2O, n = 2; L = Cl or Br, n = 4) salts when ethanolic water mixtures were employed for purification. Impure solid samples were characterized by biexponential emission decay curves.

Spectroscopic Measurements. Time-resolved and steady-state luminescence spectra were recorded by using a Nd:YAG pulsed-laser system (λ_{exc} = 355 nm, fwhm = 8 ns)[33] and a high-resolution emission spectrometer (λ_{exc} = 365 nm),[34] respectively, constructed at Michigan State University. Variable-temperature luminescence and lifetime measurements were recorded on samples cooled with an Air Products closed-cycle cryogenic system by methods described elsewhere.[33] Quantum yields of powdered samples were determined by the technique reported for solids which relies on the intensity difference between the light reflected from the sample and that reflected from a nonabsorbing MgO standard.[35] The 365-nm excitation wavelength was selected with the double monochromator of the emission spectrometer in conjunction with an Oriel 365-nm (Model 56430) interference filter. The slit widths for the monochromators filtering the excitation and emitted light were 5 mm/5 mm and 3 mm/3 mm, respectively. The entrance slit of the emission monochromator was equipped with a Schott OG-560 cutoff filter. All spectra were corrected for the instrument response function of the spectrometer as previously described.[33] Absolute quantum yields were determined by using $Ru(bpy)_3(ClO_4)_2$ as a luminescence standard. The error associated with the measurement of solid-state quantum yields by this method is estimated to be ±30%. Unpolarized excitation spectra were recorded on a Perkin-Elmer MPF-66 emission spectrometer housed in the Jet Propulsion Laboratories and employed optically dilute (OD/cm < 0.2 at the excitation wavelength) solutions. Excitation spectra were detected at emission wavelengths of 690 or 700 nm and were corrected by using manufacturer supplied software. The spectrometer's slit width was 5 mm, and all excitation spectra employed a 610-nm cutoff filter on the emission side of the spectrometer. Samples for these measurements were contained in quartz EPR tubes that were immersed in liquid nitrogen contained in a finger Dewar flask.

Electronic absorption spectra were recorded on either a Cary 17 or a Varian 2300 UV–vis–near-IR spectrometer. Low-temperature absorption and emission measurements employed a 1:1 mixture of saturated aqueous LiCl and 1 M HCl(aq). Prior to all experiments, the solvent mixture was placed into a 1-cm quartz cuvette and subjected to five freeze–pump–thaw cycles. Low-temperature absorption measurements were achieved by placing the cuvette into a small liquid-nitrogen Dewar flask equipped with three quartz windows (1.7-cm diameter). The LiCl/HCl solvent mixture forms excellent glasses at 77 K. Emission spectra recorded at temperatures above the glassing transition temperature of the LiCl/HCl solvent mixture were measured on samples cooled in ethyl ether/dry ice (173 K) or n-pentane/liquid nitrogen (143 K) cold baths.

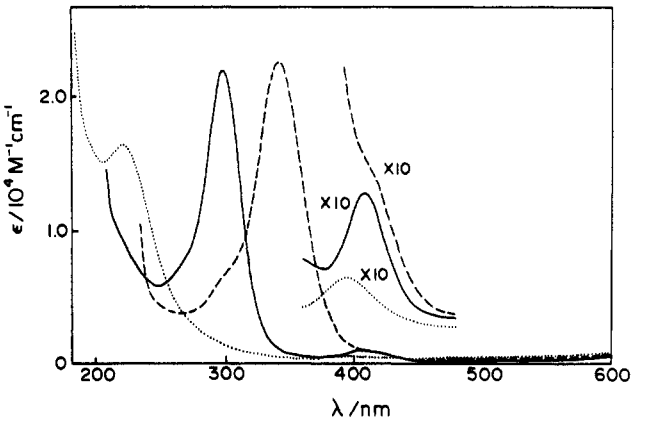

Figure 1. Solution electronic absorption spectra of $Pt_2(HPO_4)_4(H_2O)_2^{2-}$ (···) in aqueous solution and $Pt_2(HPO_4)_4Cl_2^{4-}$ (—) and $Pt_2(HPO_4)_4Br_2^{4-}$ (- - -) in 50% saturated KX(aq) solution at 300 K.

Results and Discussion

The UV–vis absorption spectra of the $Pt^{III}_2(HPO_4)_4L_2^{n-}$ complexes, shown in Figure 1, accord well with those previously reported.[31] The spectra are dominated by an intense band in the 220–350-nm spectral region and a less intense, broader band in the 390–410-nm region. This absorption profile, characteristic of d^7–d^7 complexes,[1a,3,36,37] closely parallels that of the Pt_2-

(19) Seder, T. A.; Church, S. P.; Weitz, E. *J. Am. Chem. Soc.* **1986**, *108*, 7518.
(20) (a) Kobayashi, T.; Ohtani, H.; Noda, H.; Teratani, S.; Yamazaki, H.; Yasufuku, K. *Organometallics* **1986**, *5*, 110. (b) Kobayashi, T.; Yasufuku, K.; Iwai, J.; Yesaka, H.; Noda, H.; Ohtani, H. *Coord. Chem. Rev.* **1985**, *64*, 1. (c) Yesaka, H.; Kobayashi, T.; Yasufuku, K.; Nagakura, S. *J. Am. Chem. Soc.* **1983**, *105*, 6249.
(21) Freedman, A.; Bersohn, R. *J. Am. Chem. Soc.* **1978**, *100*, 4116.
(22) Church, S. P.; Hermann, H.; Grevels, F.-W.; Schaffner, K. *J. Chem. Soc., Chem. Commun.* **1984**, 785.
(23) Coville, N. J.; Stolzenberg, A. M.; Muetterties, E. L. *J. Am. Chem. Soc.* **1983**, *105*, 2499.
(24) Wrighton, M. S.; Ginley, D. S. *J. Am. Chem. Soc.* **1975**, *97*, 2065.
(25) Rothberg, L. J.; Cooper, N. J.; Peters, K. S.; Vaida, V. *J. Am. Chem. Soc.* **1982**, *104*, 3536.
(26) Stiegman, A. E.; Miskowski, V. M.; Gray, H. B. *J. Am. Chem. Soc.* **1986**, *108*, 2781.
(27) Dulebohn, J. I.; Ward, D. L.; Nocera, D. G. *J. Am. Chem. Soc.* **1988**, *110*, 4054.
(28) Stiegman, A. E.; Miskowski, V. M. *J. Am. Chem. Soc.* **1988**, *110*, 4053.
(29) (a) Chang, I.-J.; Nocera, D. G. *J. Am. Chem. Soc.* **1987**, *109*, 4901. (b) Chang, I.-J.; Nocera, D. G. *Inorg. Chem.* **1989**, *28*, 4309. (c) Partigianoni, C. M.; Chang, I.-J.; Nocera, D. G. *Coord. Chem. Rev.* **1990**, *97*, 105.
(30) (a) Cotton, F. A.; Falvello, L. R.; Han, S. *Inorg. Chem.* **1982**, *21*, 1709. (b) Bancroft, D. P.; Cotton, F. A.; Falvello, L. R.; Han, S.; Schwotzer, W. *Inorg. Chim. Acta* **1984**, *87*, 147.
(31) El-Mehdawi, R.; Bryan, S. A.; Roundhill, D. M. *J. Am. Chem. Soc.* **1985**, *107*, 6282.
(32) Muraveiskaya, G. S.; Abashkin, V. E.; Evstaf'eva, O. N.; Golovaneva, I. F.; Shchelokov, R. N. *Sov. J. Coord. Chem. (Engl. Trans.)* **1981**, *6*, 218.
(33) Newsham, M. D.; Giannelis, E. P.; Pinnavaia, T. J.; Nocera, D. G. *J. Am. Chem. Soc.* **1988**, *110*, 3885.
(34) Mussell, R. D.; Nocera, D. G. *J. Am. Chem. Soc.* **1988**, *110*, 2764.
(35) Wrighton, M. S.; Ginley, D. S.; Morse, D. L. *J. Phys. Chem.* **1974**, *78*, 2229.
(36) Lever, A. B. P. *Inorganic Electronic Spectroscopy*; Elsevier: New York, 1984; Chapter 7.
(37) Miskowski, V. M.; Gray, H. B. In *Understanding Molecular Properties*; Avery, J., Dahl, J. P., Eds.; Reidel: Dordrecht, Holland, 1987; p 1.

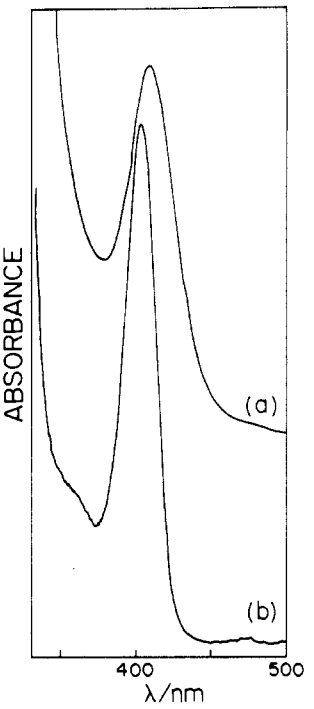

Figure 2. Electronic spectra of the low-energy absorption region of $Pt_2(HPO_4)_4Cl_2^{4-}$ in a 1:1 mixture of saturated aqueous LiCl and 1 M HCl at (a) 300 K and (b) 77 K.

$(SO_4)_4L_2^{n-}$ and $Pt_2(pop)_4L_2^{n-}$ (L = H_2O, n = 2; L = Cl or Br, n = 4) ions.[37-39] Spectroscopic studies combined with results of molecular structure determinations of several diplatinum(III) pyrophosphite complexes have led to a $\sigma \rightarrow d\sigma^*$ assignment for the intense UV absorption band.[40-42] The pronounced shift of this band toward lower energy along the axial ligand series H_2O > Cl > Br is indicative of the σ orbital possessing significant ligand character. Accordingly, it has recently been proposed that the lowest energy $\sigma \rightarrow d\sigma^*$ system in diplatinum(III) pyrophosphites is most appropriately designated $\sigma(L) \rightarrow d\sigma^*$.[43] This assignment is especially satisfying for the intense UV absorption band of $Pt^{III}_2(HPO_4)_4L_2^{n-}$ complexes because the interaction between the diplatinum(III) core and the axial ligands is weak despite the significant dependence of this band on the nature of the axial ligand. X-ray crystallographic studies have shown that the Pt–Pt bond distance is not greatly influenced by ligands in axial coordination sites.[30,44,45] Moreover, kinetic studies reveal the axial ligands to be coordinated weakly to the diplatinum core.[31,46] In this regard, it is unreasonable to expect that axial ligand mixing into the $d\sigma$ orbitals could account for the dramatic shifts observed in the absorption spectra of Figure 1.

Alternatively, the $d\sigma \rightarrow d\sigma^*$ transition of the $Pt^{III}_2(HPO_4)_4^{n-}$ complexes most likely lies to higher energy. The $d\sigma \rightarrow d\sigma^*$ transition of $Pt_2(pop)_4L_2^{n-}$ (L = H_2O, n = 2; L = Cl or Br, n = 4) ions has been observed at ~215 nm.[41] Owing to the much shorter Pt–Pt bond distances of $Pt^{III}_2(HPO_4)_4^{n-}$ complexes as compared to the pyrophosphite complexes (d(Pt–Pt) = 2.695–2.782 Å for pyrophosphites; d(Pt–Pt) = 2.486–2.592 Å for tetraphosphates),[39,44-49] a larger $d\sigma \rightarrow d\sigma^*$ splitting should result from better overlap of the Pt d_{z^2} orbitals. By use of the energy of the $d\sigma \rightarrow d\sigma^*$ absorption of $Pt^{III}_2(pop)_4L_2^{n-}$ ions as a benchmark, the $d\sigma \rightarrow d\sigma^*$ transition of the $Pt^{III}_2(HPO_4)_4^{n-}$ complexes should lie in the vacuum ultraviolet spectral region.

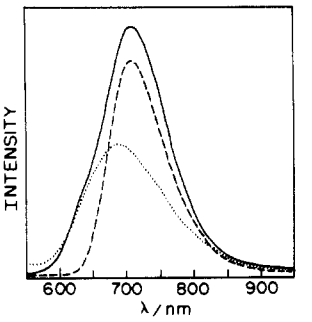

Figure 3. Corrected electronic emission spectra at 10 K of crystalline $K_nPt_2(HPO_4)_4L_2$: L = H_2O, n = 2 (···); L = Cl, n = 4 (—); L = Br, n = 4 (- - -).

Table I. Emission Spectral Data for $Pt^{III}_2(HPO_4)_4L_2^{n-}$ Complexes

$K_nPt_2(HPO_4)_4L_2$	at 10 K		at 290 K	
L/n	$\lambda_{em,max}$/nm	τ/μs	$\lambda_{em,max}$/nm	τ/μs
H_2O/2	688	1.2	678	0.33
Cl/4	710	35	694	0.71
Br/4	710	37	702	0.39

In contrast to the UV transition, the lower energy, less intense absorption system of the $Pt^{III}_2(HPO_4)_4^{n-}$ complexes (L = H_2O, Cl, Br), for the most part, is insensitive to axial ligation. The HOMOs of most d^7–d^7 D_{4h} complexes are of π or δ symmetries formed from the bonding and antibonding combinations of the (d_{xz}, d_{yz}) and d_{xy} orbitals, respectively, on each metal. Lower energy absorptions, analogous to those in Figure 1, in the spectra of diplatinum(III) pyrophosphites[40] and dirhodium(II) acetates[1a] and isocyanides[1b] have been assigned to the allowed $d\pi^* \rightarrow d\sigma^*$ transition. In agreement with electronic structural calculations,[50] the $d\delta^* \rightarrow d\sigma^*$ transition for each of these systems has been observed to lie 1500–2500 cm^{-1} to lower energy of the $d\pi^* \rightarrow d\sigma^*$ transition.[1,40,42] Conversely, absorption spectra of low-temperature glasses of $Pt_2(HPO_4)_4Cl_2^{4-}$ display a distinct band, which on the basis of energy and intensity considerations is consistent with a $d\delta^* \rightarrow d\sigma^*$ assignment, lying ~2300 cm^{-1} to higher energy of the $d\pi^* \rightarrow d\sigma^*$ transition (Figure 2). This result is not surprising in view of the fact that the much shorter Pt–Pt distance of the phosphate complexes will be manifested in a larger "$d\pi$" splitting and consequently a more destabilized $d\pi^*$ level than that typically found for d^7–d^7 complexes.

Excitation with frequencies coincident with the absorption manifold of solids and low-temperature glasses of $Pt^{III}_2(HPO_4)_4L_2^{n-}$ complexes results in strong red luminescence (Figure 3). The emissions are long-lived, and their energies are relatively insensitive to the nature of the axial ligand (Table I). Emission spectra exhibit no vibrational fine structure and remain featureless at temperatures as low as 10 K. The half-width of the emission band is temperature dependent, increasing for example from 1114 to 1471 cm^{-1} between 10 and 290 K for $K_4Pt_2(HPO_4)_4Cl_2$, but much less than that reported for the $d\sigma^* \rightarrow d\sigma$ emission band of $Re_2(CO)_6(dmpm)_2$ (dmpm = bis(dimethylphosphino)methane).[28]

(38) Bryan, S. A.; Schmehl, R. H.; Roundhill, D. M. *J. Am. Chem. Soc.* **1986**, *108*, 5408.
(39) Roundhill, D. M.; Gray, H. B.; Che, C.-M. *Acc. Chem. Res.* **1989**, *22*, 55.
(40) Che, C.-M.; Butler, L. G.; Grunthaner, P. J.; Gray, H. B. *Inorg. Chem.* **1985**, *24*, 4662.
(41) Isci, H.; Mason, W. R. *Inorg. Chem.* **1985**, *24*, 1761.
(42) Che, C.-M.; Lee, W.-M.; Mak, T. C. W.; Gray, H. B. *J. Am. Chem. Soc.* **1986**, *108*, 4446.
(43) Che, C.-M.; Mak, T. C. W.; Miskowski, V. M.; Gray, H. B. *J. Am. Chem. Soc.* **1986**, *108*, 7840.
(44) (a) Conder, H. L.; Cotton, F. A.; Falvello, L. R.; Han, S.; Walton, R. A. *Inorg. Chem.* **1983**, *22*, 1887. (b) Cotton, F. A.; Han, S.; Conder, H. L.; Walton, R. A. *Inorg. Chim. Acta* **1983**, *72*, 191.
(45) El-Mehdawi, R.; Fronczek, F. R.; Roundhill, D. M. *Inorg. Chem.* **1986**, *25*, 3714.
(46) El-Mehdawi, R.; Fronczek, F. R.; Roundhill, D. M. *Inorg. Chem.* **1986**, *25*, 1155.
(47) Che, C.-M.; Schaefer, W. P.; Gray, H. B.; Dickson, M. K.; Stein, P. B.; Roundhill, D. M. *J. Am. Chem. Soc.* **1982**, *104*, 4253.
(48) Woollins, J. D.; Kelly, P. F. *Coord. Chem. Rev.* **1985**, *65*, 115.
(49) (a) Hedden, D.; Roundhill, D. M.; Walkinshaw, M. D. *Inorg. Chem.* **1985**, *24*, 3146. (b) Alexander, K. A.; Bryan, S. A.; Fronczek, F. R.; Fultz, W. C.; Rheingold, A. L.; Roundhill, D. M.; Stein, P.; Watkins, S. F. *Inorg. Chem.* **1985**, *24*, 2803.
(50) (a) Norman, J. G.; Renzoni, G. E.; Case, D. A. *J. Am. Chem. Soc.* **1979**, *101*, 5256. (b) Norman, J. G.; Kolari, H. J. *J. Am. Chem. Soc.* **1978**, *100*, 791.

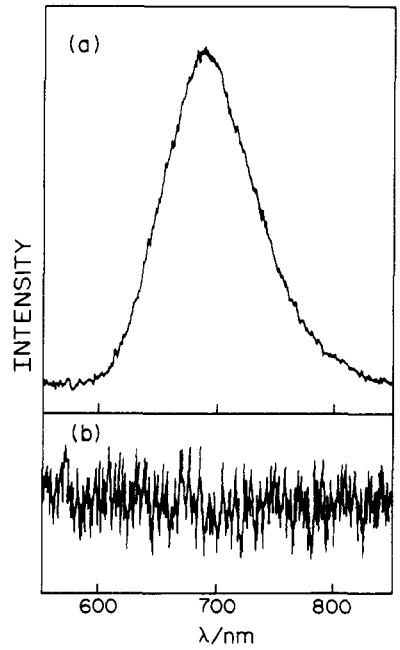

Figure 4. (a) Electronic emission from $Pt_2(HPO_4)_4Cl_2^{4-}$ in a low-temperature glass (77 K) of saturated LiCl(aq) and 1 M HCl. (b) Scan over the same spectral region of the same solution at a temperature (143 K) just above the glassing transition. This scan was recorded at 10 times the sensitivity of that used for scan a.

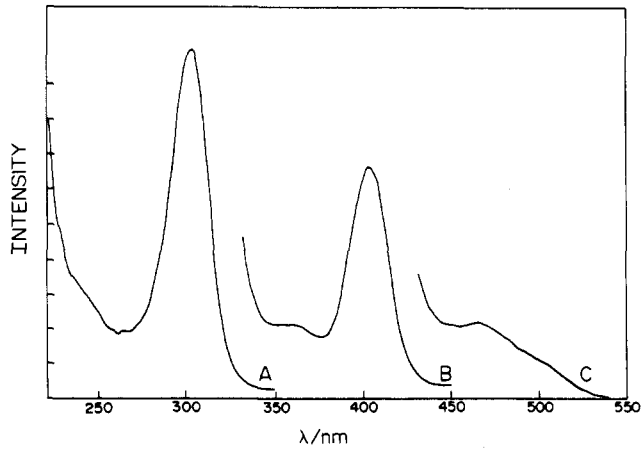

Figure 5. Unpolarized excitation spectra of $Pt_2(HPO_4)_4Cl_2^{4-}$ in low-temperature glasses (77 K) of 1:1 saturated LiCl(aq)/1 M HCl. Progressively more concentrated solutions were used in order to obtain adequate signal to noise ratios for the spectral regions A, B, and C. In each case OD/cm was maintained <0.2 within the spectral region being studied.

Although luminescence from crystalline $Pt^{III}_2(HPO_4)_4L_2^{n-}$ complexes is detected over a wide temperature range, solutions of these complexes do not luminesce. This behavior is most vividly demonstrated by the results reproduced in Figure 4. Frozen glasses of $K_4Pt_2(HPO_4)_4Cl_2$ are intensely luminescent. However, luminescence is not detected from solutions at temperatures just above the glassing transition. These observations are consistent with recent photophysical studies demonstrating the importance of medium rigidity as a crucial controlling factor of $d\sigma^*$ luminescence.[26-28]

Figure 5 displays the unpolarized excitation spectrum of low-temperature glasses of $Pt_2(HPO_4)_4Cl_2^{4-}$ at 77 K. In agreement with the observed absorption profile, excitation bands corresponding to the proposed $^1(\sigma(L) \rightarrow \sigma^*)$, $^1(d\delta^* \rightarrow d\sigma^*)$, and $^1(d\pi^* \rightarrow d\sigma^*)$ transitions are observed at 301, 360, and 403 nm, respectively. Additionally, several other features not readily discerned by absorption spectroscopy are clearly distinguished in Figure 5. Most notable is the presence of a weak multicomponent feature on the low-energy tail of the $^1(d\pi^* \rightarrow d\sigma^*)$ excitation band

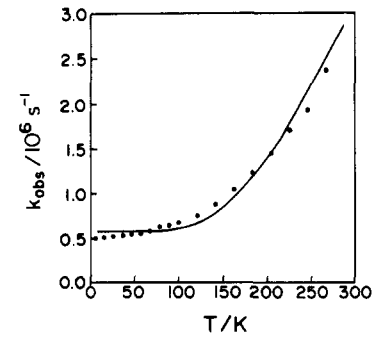

Figure 6. Fit of the variation of the observed emission decay rate constant of $K_2Pt_2(HPO_4)_4(H_2O)_2$ to eq 1 in the 10–290 K temperature range.

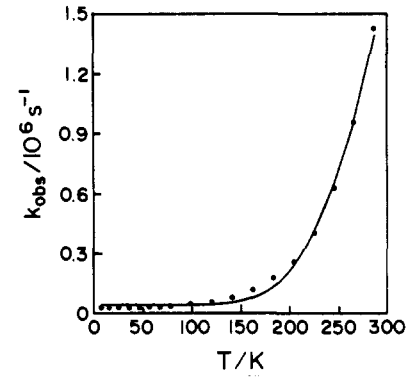

Figure 7. Fit of the variation of the observed emission decay rate constant of $K_4Pt_2(HPO_4)_4Cl_2$ to eq 1 in the 10–290 K temperature range.

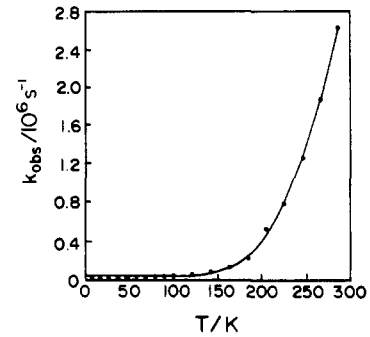

Figure 8. Fit of the variation of the observed emission decay rate constant of $K_4Pt_2(HPO_4)_4Br_2$ to eq 1 in the 10–290 K temperature range.

that resolves into a 465-nm maximum and a 505-nm shoulder in spectra recorded on concentrated glasses of $Pt_2(HPO_4)_4Cl_2^{4-}$. The 3000–5000-cm^{-1} red shift of these weak features from the $^1(d\pi^* \rightarrow d\sigma^*)$ transition are of the appropriate magnitude for singlet–triplet splittings. In the absence of spin–orbit coupling only one transition, $^3E_u \leftarrow {}^1A_{1g}$, is expected to arise from the one-electron $^3(d\pi^* \rightarrow d\sigma^*)$ promotion. However, the ^3E_u excited state in D_{4h} symmetry is 6-fold degenerate and in the presence of a spin–orbit coupling perturbation will decompose into A_{1u}, A_{2u}, B_{1u}, B_{2u}, and E_u symmetries in the D_{4h}' double group.[51] First-order spin–orbit coupling calculations show that the degeneracy of the (A_{1u}, A_{2u}) and (B_{1u}, B_{2u}) pairs is not split and that the energy ordering of the spin–orbit components increases along the series (B_{1u}, B_{2u}) < E_u < (A_{1u}, A_{2u}).[52] Of these spin–orbit states, transitions to the E_u and A_{2u} states are dipole-allowed and are expected to carry

(51) Winkler, J. R.; Gray, H. B. *Inorg. Chem.* **1985**, *24*, 346.

(52) The three $d\pi^* \rightarrow d\sigma^*$ assignments, $A_{2u}(^3E_u) \leftarrow {}^1A_{1g}$, $E_u(^3E_u) \leftarrow {}^1A_{1g}$, and $^1E_u \leftarrow {}^1A_{1g}$, were fit to the spin–orbit coupling matrix to yield zero-order energies of 20 177 and 24 499 cm^{-1} for the ^3E_u and ^1E_u states, respectively, and a reasonable[51] value for the spin-orbit coupling parameter λ = 2655 cm^{-1} was obtained. The energies of the spin–orbit states, to second-order, within the $^{1,3}E_u$ manifold are as follows: $\epsilon(B_{1u}) = \epsilon(B_{2u})$ = 18 850 cm^{-1}; $\epsilon(E_u(^3E_u))$ = 19 802 cm^{-1}; $\epsilon(A_{1u}) = \epsilon(A_{2u})$ = 21 504 cm^{-1}; $\epsilon(E_u(^1E_u))$ = 24 875 cm^{-1}.

Table II. Calculated Decay Rate Constants and Energy Gaps of the $Pt^{III}_2(HPO_4)_4L_2^{n-}$ Complexes[a]

$K_nPt_2(HPO_4)_4L_2$ L/n	$\Delta E/cm^{-1}$	k_1/s^{-1}	k_2/s^{-1}
$H_2O/2$	1126	5.8×10^5	2.2×10^7
Cl/4	2256	4.3×10^4	1.3×10^8
Br/4	2117	3.6×10^4	1.9×10^8

[a] Calculated from eq 1.

intensity because of singlet–triplet mixing with the energetically proximate ^1E_u (arising from the $^1(d\pi^* \rightarrow d\sigma^*)$ one-electron promotion) and $^1A_{2u}$ (arising from the $^1(\sigma(d_{z^2}, L) \rightarrow d\sigma^*)$ one-electron promotions) states. To this end, our observation of two weak transitions to lower energy of the $^1(d\pi^* \rightarrow d\sigma^*)$ band is in accordance with straightforward spin–orbit considerations, and we assign the 465-nm and 505-nm excitation bands to the $A_{2u}(^3E_u) \leftarrow {}^1A_{1g}$ and $E_u(^3E_u) \leftarrow {}^1A_{1g}$ transitions, respectively.

In order to further elucidate the dynamics of the $d\sigma^*$ excited state, a detailed study of the temperature dependence of the luminescence was initiated after observing a pronounced attenuation of emission from crystalline $Pt^{III}_2(HPO_4)_4L_2^{n-}$ complexes with increasing temperature. Figures 6–8 display the temperature dependences of the exicted state decay rate constants of the potassium salts of $Pt_2(HPO_4)_4(H_2O)_2^{2-}$, $Pt_2(HPO_4)_4Cl_2^{4-}$, and $Pt_2(HPO_4)_4Br_2^{4-}$, respectively; for all experiments, monoexponential decay of the emission was observed. An issue of principal interest is the temperature dependence of the $Pt^{III}_2(HPO_4)_4L_2^{n-}$ emission lifetimes. In each figure, a temperature regime in which the decay rate constant exhibits little variance is followed by a sharp monotonic increase of the rate with increasing temperature. These data clearly demonstrate the presence of a thermally accessible decay channel. As indicated by the solid lines in Figures 6–8, the observed rates are fit extremely well by an expression for the decay constant based on a two-state Boltzmann distribution

$$k_{obs} = \frac{k_1 + k_2 \exp(-\Delta E/k_B T)}{1 + \exp(-\Delta E/k_B T)} \quad (1)$$

where k_1 and k_2 are the decay constants for two states in thermal equilibrium that are separated by an energy gap ΔE. Calculated rate constants and energy gaps for the $Pt^{III}_2(HPO_4)_4L_2^{n-}$ complexes are summarized in Table II. For each of the phosphate complexes, examination of the data shows that an extremely efficient decay pathway is accessed via the higher energy excited state. This observation is further quantitated by combining temperature-dependence lifetimes with measurements of the corresponding temperature-dependent quantum yields. At a given temperature, the quantum yield, Φ_e, is related to the observed lifetime by the radiative rate constant k_r, according to the well-known expression[53]

$$\Phi_e = \tau_0 k_r \quad (2)$$

from which the nonradiative decay rate k_{nr} may directly be determined

$$\tau_0 = (k_r + k_{nr})^{-1} \quad (3)$$

Over all temperatures, the nonradiative rate is 10^2–10^4 greater than that of the radiative rate. For example, representative measurements of temperature-dependent quantum yields, lifetimes, and calculated radiative and nonradiative rate constants of $K_4Pt_2(HPO_4)_4Cl_2$ are displayed in Table III. In the temperature-independent lifetime regime, k_r is 6.6 (4) $\times 10^2$ s^{-1} whereas k_{nr} is 3.3 (6) $\times 10^4$ s^{-1}; this ratio of the radiative and nonradiative rate increases to 10^4 at room temperature ($k_r = 1.8 \times 10^2$ s^{-1}, $k_{nr} = 1.4 \times 10^6$ s^{-1} at 290 K). The axially substituted water and bromide complexes exhibit behavior parallel to that of the chloride complex.[54] This significant increase in the nonradiative rate at higher temperatures is indicative of the additional contribution of this higher energy excited state to the decay of electronically excited $Pt^{III}_2(HPO_4)_4L_2^{n-}$ complexes.

Table III. Temperature-Dependent Quantum Yields, Lifetimes, and Calculated Radiative and Nonradiative Rate Constants of Crystalline $K_4Pt_2(HPO_4)_4Cl_2$

T/K	$\Phi_e/10^{-2}$	$\tau/\mu s$	$k_{nr}/10^4$ s^{-1}	$k_r/10^2$ s^{-1}
8.4	2.4	35	2.8	7.1
17	2.5	35	2.8	7.3
38	2.5	36	2.7	6.7
58	2.2	32	3.0	6.9
79	1.8	29	3.4	6.2
101	1.5	21	4.7	7.0
122	1.2	17	5.9	7.2
143	0.91	12	8.2	7.5
164	0.63	8.3	12	7.5
185	0.46	5.5	18	8.3
206	0.36	3.8	27	9.5
227	0.27	2.5	40	11
248	0.20	1.6	62	13
269	0.14	1.1	95	13
290	0.13	0.71	140	18

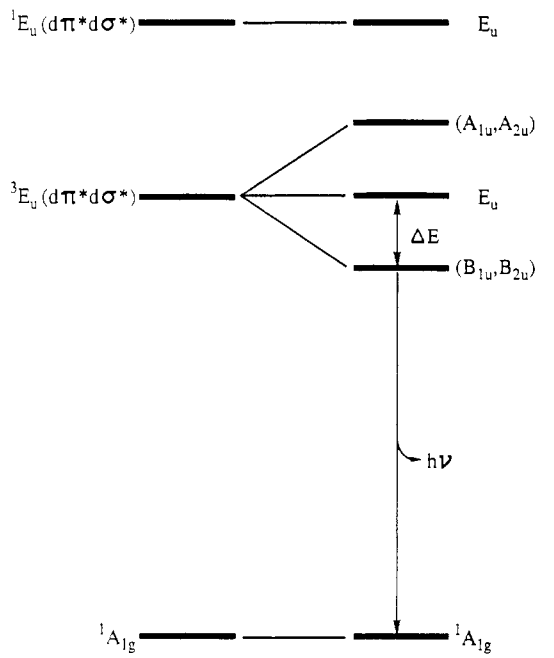

Figure 9. Proposed energy diagram of the lowest energy excited states of the $Pt^{III}_2(HPO_4)_4L_2^{n-}$ complexes. The state manifold is derived from the spin–orbit coupling perturbation of the ^3E_u state arising from the one-electron $^3(d\pi^* \rightarrow d\sigma^*)$ promotion.

An excited-state model consistent with the spectroscopic and photophysical properties of $Pt^{III}_2(HPO_4)_4L_2^{n-}$ complexes is illustrated in Figure 9. The lowest energy excited-state manifold is derived from the $d\pi^*d\sigma^*$ electronic configuration; luminescence originates from the (B_{1u}, B_{2u}) spin–orbit pair. Because there are no close-lying $^1B_{1u}$ and $^1B_{2u}$ states to configurationally mix with this pair, the emissive excited state is predicted to be nearly pure triplet in character. To this end, the model accounts nicely for the very small radiative rate constants ($k_r = 10^2$–10^3 s^{-1}) for the $Pt^{III}_2(HPO_4)_4L_2^{n-}$ series. We attribute the observed temperature dependence of the $Pt^{III}_2(HPO_4)_4L_2^{n-}$ lifetimes and emission quantum yields to thermal population of the $E_u(^3E_u)$ excited state. It is noteworthy that the energy gaps determined from temperature-dependent lifetime measurements (Table II) conform well with the (B_{1u}, B_{2u}) – E_u splitting determined from first-order spin–orbit coupling calculations.[52] The calculated 952-cm^{-1} splitting is in order of magnitude agreement with the observed energy gaps. The larger energy gaps of $Pt^{III}_2(HPO_4)_4L_2^{n-}$ complexes axially substituted by halide ligands can be accounted for by increased second-order contributions of the halides, as compared to water, to the spin–orbit coupling constant. Additionally, en-

(53) Turro, N. J. *Modern Molecular Photochemistry*; Benjamin/Cumming: Menlo Park, CA, 1978.

(54) Temperature-dependent lifetimes, temperature-dependent quantum yields, and calculated radiative and nonradiative rate constants of crystalline potassium salts of $Pt_2(HPO_4)_4(H_2O)_2^{2-}$, $Pt_2(HPO_4)_4Cl_2^{4-}$, and $Pt_2(HPO_4)_4Br_2^{4-}$ are included as supplementary material.

hanced nonradiative decay from the higher energy deactivating state is also explained by this model because intersystem crossing from the $E_u(^3E_u)$ state with respect to the lowest energy ($B_{1u}(^3E_u$, $B_{2u}(^3E_u)$) level will be promoted by the increased singlet character of the former state arising from efficient mixing with its energetically proximate singlet (vide supra). Moreover, the $E_u(^3E_u)$ state is possibly split by the Jahn-Teller effect and may therefore exhibit a larger nontotally symmetric distortion than the other spin-orbit states.[55] Such distortions are usually effective in promoting efficient nonradiative decay.

Thus, the excited-state dynamics of the $Pt^{III}_2(HPO_4)_4L_2^{n-}$ complexes clearly reveal the existence of efficient deactivation pathways of $d\sigma^*$ excited states even when metal-metal or metal-axial ligand dissociation is precluded. Our results suggest that the spin-orbit components of the $^3(d\pi^*d\sigma^*)$ configuration controls the dynamics of $d\sigma^*$ emission from the $Pt^{III}_2(HPO_4)_4L_2^{n-}$ complexes. Specifically, the $E_u(^3E_u)$ excited state proximate to the lowest energy emissive ($B_{1u}(^3E_u)$, $B_{2u}(^3E_u)$) level provides a facile decay channel to ground state. A small (B_{1u}, B_{2u}) - E_u energy gap may explain the absence of $d\sigma^*$ emission from other singly bonded metal-metal complexes. The ability to control the magnitude of this energy gap with heavy-atom donor ligands in the axial coordination sites provides the opportunity to synthetically tune the excited-state lifetime and, consequently, luminescence intensity of $d\sigma^*$ excited states.

Acknowledgment. We thank Drs. Al Stiegman and Mordechai Bixon for helpful discussions. The financial support of this work by National Science Foundation Grant CHE-8705871 (D.G.N.) is gratefully acknowledged.

Supplementary Material Available: Tables of temperature-dependent quantum yields, temperature-dependent lifetimes, and calculated radiative and nonradiative rate constants (3 pages). Ordering information is given on any current masthead page.

(55) Hopkins, M. D.; Miskowski, V. M.; Gray, H. B. *J. Am. Chem. Soc.* **1986**, *108*, 6908.

Contribution from the Department of Chemistry, Clemson University, Clemson, South Carolina 29634-1905

Competitive Hydrogen Production and Emission through the Photochemistry of Mixed-Metal Bimetallic Complexes

D. Brent MacQueen and John D. Petersen*

Received July 25, 1989

Preparation of the complexes $RhH_2(PPh_3)_2L^+$, $[RhH_2(PPh_3)_2]_2L^{2+}$, and $(bpy)_2RuLRhH_2(PPh_3)_2^{3+}$ where L is 2,2'-bipyrimidine (bpm), 2,3-bis(2-pyridyl)pyrazine (dpp), and 2,3-bis(2-pyridyl)quinoxaline (dpq), as well as the monometallic analogues $RhH_2(PPh_3)_2en^+$ and $RhH_2(PPh_3)_2bpy^+$ (en = ethylenediamine and bpy = 2,2'-bipyridine) is described. All of the complexes undergo photochemically induced reductive elimination of molecular hydrogen when irradiated at wavelengths equal to or shorter than 405 nm for the monometallic complexes and equal to or shorter than 436 nm for the bimetallic complexes. In addition, the monometallic rhodium complexes and the heterobimetallic (RuLRh) complexes undergo emission in fluid solution at room temperature from a state different than the photoactive state. In the case of the heterobimetallic complexes, the photoemissive state is best described as a Ru-based metal-to-ligand charge-transfer (MLCT) state while the photoreaction is assigned as a Rh-based ligand-field (LF) state in all of the complexes studied.

Introduction

The use of tris(bipyridine)ruthenium(II), $Ru(bpy)_3^{2+}$, as a photosensitizer has been widely exploited due to both the ion's inertness toward photosubstitution reactions and its long-lived excited state ($\tau \sim 600$ ns) at room temperature. In addition, the intense absorption feature that this complex displays in the visible region of the spectrum has made it a likely candidate for solar energy conversion studies.[2-5] $Ru(bpy)_3^{2+}$ has been used as an excited-state energy-transfer[6-9] as well as electron-transfer[10-14] reagent. The incorporation of a "$Ru(bpy)_3^{2+}$ like" chromophore into a multicomponent system to sensitize a useful photochemical reaction has been proposed in order to circumvent the inherent inefficiency of the bimolecular collision process used to facilitate energy or electron transfer in the previous photochemical systems.

Intramolecular energy transfer has been observed in numerous inorganic photochemical systems; however, most of the reported systems involve energy transfer from an intraligand transition (IL) to a ligand-field (LF) state from which photochemistry is observed.[15-17] The examples of energy transfer from a metal-to-ligand charge-transfer (MLCT) transition localized on one metal center to an LF or MLCT excited state of a covalently attached metal center are recent and few.[18-23]

The complexes $Ru(bpy)_2L^{2+}$ and $[Ru(bpy)_2]_2L^{4+}$, where L = 2,3-bis(2-pyridyl)pyrazine (dpp), 2,3-bis(2-pyridyl)quinoxaline

(1) Van Houten, J.; Watts, R. J. *J. Am. Chem. Soc.* **1976**, *98*, 4853.
(2) Kalyanasundaram, K. *Coord. Chem. Rev.* **1982**, *46*, 159.
(3) Kirch, M.; Lehn, J.; Sauvage, J. *Helv. Chim. Acta* **1979**, *62*, 1345.
(4) Juris, A.; Balzani, V.; Barigelletti, F.; Campagna, S.; Belser, P.; Von Zelewsky, A. *Coord. Chem. Rev.* **1988**, *84*, 85.
(5) Balzani, V., Ed. *Supramolecular Photochemistry*; NATO ASI Series C; D. Reidel: The Netherlands, 1987; Vol. 214.
(6) Lin, C.-T.; Böttcher, W.; Chou, M.; Creutz, C.; Sutin, N. *J. Am. Chem. Soc.* **1976**, *98*, 6536.
(7) Sabbatini, N.; Balzani, V. *J. Am. Chem. Soc.* **1972**, *94*, 7587.
(8) Demas, J. N.; Adamson, A. W. *J. Am. Chem. Soc.* **1971**, *93*, 1800.
(9) Kane-Maguire, N. A. P.; Langford, C. H. *J. Am. Chem. Soc.* **1972**, *94*, 2125.
(10) Navon, G.; Sutin, N. *Inorg. Chem.* **1974**, *13*, 2159.
(11) Gafney, H. D.; Adamson, A. W. *J. Am. Chem. Soc.* **1972**, *94*, 8238.
(12) Bock, C. R.; Meyer, T. J.; Whitten, D. G. *J. Am. Chem. Soc.* **1974**, *96*, 4710.
(13) Sutin, N.; Creutz, C. *Adv. Chem. Ser.* **1978**, *No. 168*, 1.
(14) Meyer, T. J. *Acc. Chem. Res.* **1978**, *11*, 94.
(15) Adamson, A. W.; Vogler, A.; Lantzke, I. *J. Phys. Chem.* **1969**, *73*, 4183.
(16) Bergkamp, M. A.; Watts, R. J.; Ford, P. C. *Inorg. Chem.* **1981**, *20*, 1764.
(17) Hennig, H.; Rehorek, D. *Coord. Chem. Rev.* **1985**, *61*, 1.
(18) Gelroth, J. A.; Figard, J. E.; Petersen, J. D. *J. Am. Chem. Soc.* **1979**, *101*, 3649.
(19) Moore, K. J.; Lee, L.; Figard, J. E.; Gelroth, J. A.; Stinson, A. J.; Wohlers, H. D.; Petersen, J. D. *J. Am. Chem. Soc.* **1983**, *105*, 2274.
(20) Nishizawa, M.; Ford, P. C. *Inorg. Chem.* **1981**, *20*, 2016.
(21) Schmehl, R. H.; Auerbach, R. A.; Wacholtz, W. F.; Elliott, C. M.; Freitag, R. A.; Merkert, J. W. *Inorg. Chem.* **1986**, *25*, 2440.
(22) Wacholtz, W. F.; Auerbach, R. A.; Schmehl, R. H. *Inorg. Chem.* **1987**, *26*, 2989.
(23) Schmehl, R. H.; Auerbach, R. A.; Wacholtz, W. F. *J. Phys. Chem.* **1988**, *92*, 6202.

0020-1669/90/1329-2313$02.50/0